BIOCHEMISTRY
including biophysical chemistry & molecular biology
Article

Biochemistry **2009,** *48,* 8233–8240 8233
DOI: 10.1021/bi900342d

Local and Global Effects of a Cavity Filling Mutation in a Metastable Serpin†

Tanusree Sengupta, Yuko Tsutsui, and Patrick L. Wintrode*

Department of Physiology & Biophysics, Case Western Reserve University, Cleveland, Ohio 44106

Received May 27, 2009; Revised Manuscript Received July 21, 2009

ABSTRACT: The serpins are an unusual class of protease inhibitors which fold to a metastable form and subsequently undergo a massive conformational change to a stable form when they inhibit their target proteases. The driving force for this conformational change has been extensively investigated by site directed mutagenesis, and it has been found that mutations which stabilize the metastable form frequently result in activity deficiency. Here, we employ hydrogen/deuterium exchange to probe the effects of a cavity filling mutant of α_1AT. The Gly117 → Phe substitution fills a cavity between the F-helix and the face of β-sheet A, stabilizes the metastable form of α_1AT by ~4 kcal/mol and results in a 60% reduction in inhibitory activity against elastase. Globally, the G117F substitution alters the unfolding mechanism by eliminating the molten globule intermediate that is seen in wild type unfolding. Remarkably, this is accomplished primarily by destabilizing the molten globule rather than stabilizing the metastable native state. Locally, conformational flexibility in the native state is reduced in specific regions: the top of the F-helix, β-strands 5A, 1C, and 4C, and helix D. Except for strand 4C, all of these regions mediate or propagate conformational changes. The F-helix and strand 5A must be displaced during protease inhibition, displacement of strand 1C is required for polymer formation, and helix D is a site (in antithrombin) of allosteric regulation. Our results indicate that these functionally important regions form a delocalized network of residues that are dynamically coupled and that both local and global stability mediate inhibitory activity.

The native state of most globular proteins is the conformation with the lowest Gibbs free energy. However, for some proteins an energy barrier prevents them from adopting the lowest free energy state, thus trapping them in a metastable state. Some typical examples are the membrane fusion proteins of some viruses, α-lytic proteases, arrestin, and serpins. Serpins are a large and widely distributed family of serine protease inhibitors which include plasma protease inhibitors such as α_1-antitrypsin (α_1AT[1]), α_1-antichymotrypsin, antithrombin III, plasminogen activator inhibitor-I, and C1 inhibitor as well as noninhibitory members such as ovalbumin and angiotensinogen (*1*). Inhibitory serpins share a common tertiary structure consisting of three β sheets (A, B, and C) and 8 to 9 helices, with the extended reactive center loop exposed at one end of the molecule for protease binding (Figure 1A) (*2*). Upon cleavage by a protease, the amino terminal portion of the cleaved reactive center loop (RCL) of the serpin inserts into the central β sheet A with the protease covalently linked to it (*3*). This conformational transition from stressed (S) (also referred to as native) form to relaxed (R) form results in a dramatic increase in thermal stability of the molecule (*4*). Unfavorable interactions in the native form such as side-chain overpacking, buried polar groups, and cavities present in the serpin molecule have been identified as the structural basis for native metastability (*5*−*8*), and such metastability thus turns out to be absolutely crucial for efficient protease inhibitor activity. The metastability of serpins and their ability to undergo controlled conformational changes also rendered these molecules able to convert to a latent inactive state (*3*). In the latent form, the RCL of the serpin molecule inserts into β-sheet A and therefore cannot react with the target protease. This also makes them vulnerable to misfolding and polymerization (*9*).

Extensive mutagenesis studies have probed the role of local and global stability in serpins (*10*−*14*). Single stabilizing mutations near the RCL and in β-sheet A result in decreased activity, indicating that local instability in these regions is important for function (*10*−*12*). However, it has been shown that combinations of multiple stabilizing mutations can compromise activity regardless of location, provided that the degree of stabilization exceeds a threshold of ~13 kcal/mol (*14*). From these studies, it appears that both local and global instability contribute to serpin function. One drawback to these studies is that, while they determined the effect of mutations on the stability of α_1AT, they did not investigate their effect on conformational flexibility, which is also expected to play a role in inhibitory function.

Recently, the local distribution of both stability and conformational flexibility in α_1AT was investigated using hydrogen/deuterium exchange and mass spectrometry (*15*, *16*). Conformational flexibility was found to vary widely between different regions, for example, the top of the F-helix is extremely labile, while most of the β-sheets A and B are rigid (*15*). In contrast, stability was much more uniformly distributed. The entire molecule undergoes a concerted transition to a molten globule state at 0.8 M GdnHCl, while the ΔG of unfolding for all regions clustered around a value of 5 kcal/ mole (*16*).

In the present study, we have employed HXMS to study the local dynamics and local/global unfolding in a mutant of α_1AT in which glycine 117 has been substituted with phenylalanine.

†This work was supported by NIH grant R01HL085469.
*Corresponding author. Phone: (216) 368-3178. Fax: (216) 368-3952. E-mail: patrick.wintrode@case.edu.
[1]Abbreviations: α_1AT, α_1-antitrypsin; HXMS, hydrogen/deuterium exchange/mass spectrometry; CD, circular dichroism; G117F, Gly117 → Phe.

Published on Web 07/22/2009

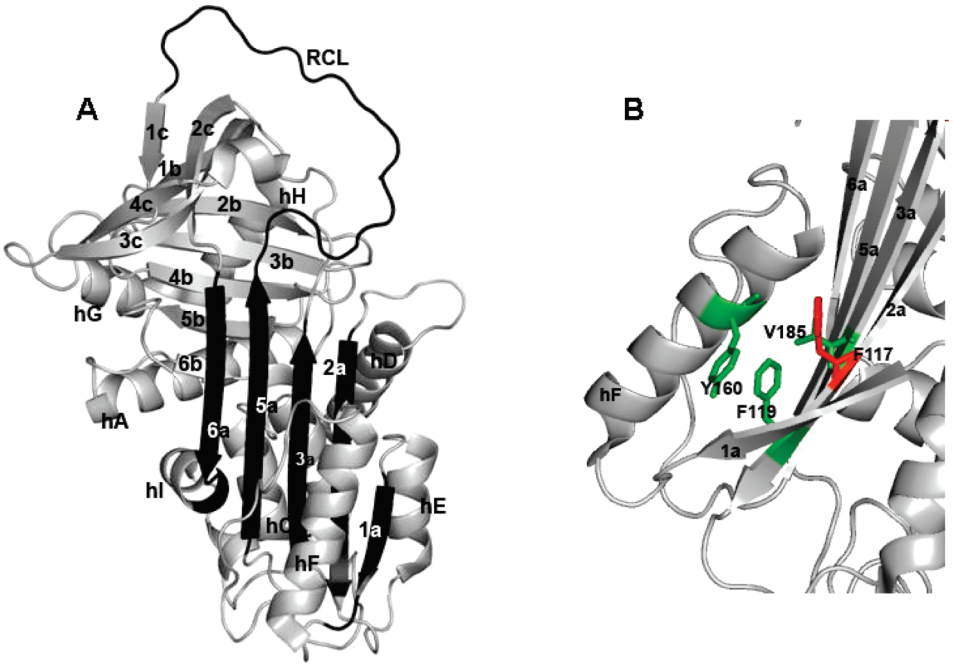

FIGURE 1: (A) Structure of the metastable form of α_1AT. β-sheet A is shown in black, and other functionally significant regions are indicated with arrows. (B) Close up view of the structure of G117F (*21*). Phe117 is shown in red, and the surrounding residues are shown in green. The figures were prepared using PyMol (*38*).

Gly 117 is on β-sheet 2A, and the C^{α} of the residue is surrounded by Phe-119, Tyr-160, and Val-185 on the outer face of β-sheet A (Figure 1B). This site forms a cavity that can accommodate larger side chains without appreciably altering the main structure. Substitution of Gly by the larger hydrophobic residue Phe fills a cavity between helix F and β-sheet A, and this substitution was shown to both increase the thermodynamic stability of α_1AT and to reduce its inhibitory activity toward elastase (*12*). As the rate of association with elastase was unchanged, it was assumed that activity loss resulted from reduced efficiency of RCL translocation and insertion. Using this mutant, we tried to further elucidate the respective roles of conformational flexibility and stability in serpin function.

MATERIALS AND METHODS

Protein Expression, Purification, and Activity of G117F. The mutant protein was expressed and purified as described earlier (*15*). Activity assay of α_1AT was performed against trypsin (sigma) and elastase as described (*12*, *15*). Because active site titrants of porcine pancreatic elastase (PPE) are not readily available, absolute activity was not determined. However, wild type and G117F assays were performed simultaneously against the same preparation of trypsin or PPE, and therefore, the relative activity values are accurate.

Peptide Mapping by HPLC MS/MS. Peptide mapping was performed as described before (*15*). In short, 5 μg of G117F in 10 mM sodium phosphate (pH 7.8) and 50 mM NaCl (Buffer A) was digested with 5 μg of porcine pepsin dissolved in 0.05% (v/v) TFA and incubated for 5 min on ice. The digested protein was injected into a micropeptide trap (Michrom Bioresources) connected to a C18 HPLC column (5 cm × 1 mm, Altech) coupled to a Finnigan LCQ quadrupole ion-trap mass spectrometer (ThermoElectron) for the sequencing of each peptic peptide.

Equilibrium Unfolding by H/D Exchange. Five micrograms of the protein was incubated in buffer A containing different concentrations of GdnHCl for 1 h at room temperature. The sample was then 10-fold diluted with 10 mM sodium phosphate (pD 7.8) and 50 mM NaCl in D_2O buffer containing the same concentration of Gdn^2HCl as the preincubation sample. The exchange reaction was allowed to proceed for 10 s at room temperature followed by the addition of 100 mM NaH_2PO_4 (pH 2.4) as the quench buffer. The final protein concentration was 0.5 μM. The quenched sample was then quickly frozen in a dry ice/ethanol bath and stored at −80 °C. The concentration of GdnHCl and $GdnH^2Cl$ were determined by refractometry.

Conformational Dynamics Study by H/D Exchange. Five micrograms of the protein in buffer A was 24 times diluted with the same buffer prepared in D_2O at room temperature to label the sample. H/D exchange was terminated at different time points by the addition of the quench buffer (100 mM NaH_2PO_4 at pH 2.4) and quickly frozen in a dry ice/ ethanol bath. The final protein concentration was the same as that in the equilibrium study. The samples were kept at −80 °C until use.

Isotope Analysis of HPLC Electrospray Ionization (ESI). The frozen samples were quickly thawed and digested with 5 μg of porcine pepsin for 5 min. The digested sample was quickly injected into a micropeptide trap connected to a C18 HPLC column coupled to a Finnigan LCQ quadrupole ion-trap mass spectrometer. Peptides were eluted in 12 min using a gradient of 10−45% acetonitrile at a flow rate of 50 μL/ min. The micropeptide trap and column were all immersed in ice during the experiment to minimize back exchange.

Analyses of the unfolding curves were done according to the method described in ref *16*. Percent deuterium exchange at different points was calculated as described previously (*15*).

Equilibrium Unfolding in GdnHCl by CD Spectroscopy. CD spectra were obtained using an Aviv 215 series CD spectrometer at 25 °C with 1 nm/10 s signal averaging from 210 to 250 nm using a 1 mm path-length cell. The protein was incubated in buffer A containing different concentrations of optical-grade GdnHCl (Pierce) for 1 h at 25 °C. The equilibrium unfolding curve was determined from the signal at 222 nm as a function of

the concentration of denaturant. The data were fitted to a two state unfolding equation.

RESULTS

The inhibitory activity of G117F against bovine trypsin was found to be 20% less than that of wild type. This is a smaller reduction than the 55−60% decrease seen against porcine pancreatic elastase that is reported in this work and elsewhere (*12*), but larger than the negligible change in activity seen against chymotrypsin (*17*).

Equilibrium unfolding of wild type α_1AT by acid or chemical denaturants follows a three state transition model as revealed by CD spectroscopy (*18*−*20*). The biphasic nature of the wild type unfolding curve in Figure 2 indicates the presence of an intermediate. The unfolding profile for the mutant G117F was found to be different from that of the wild type. The far-UV CD spectral data showed a two state transition with the transition midpoint at 1.4 M GdnHCl (Figure 2). The nature of the unfolding curve and transition midpoint of G117F were in good agreement with that found previously using fluorescence spectroscopy (*12*). The transition midpoint of 1.4 M is slightly higher than the midpoint of ~1.2 M found in ref *12*, but this small difference may be due to the difference in pH (pD 7.8 in this study; pH 6.5 in ref *12*) as well as to the fact that unfolding was monitored by different techniques. For wild type α_1AT, intrinsic tryptophan fluorescence spectroscopy indicates two state unfolding (*12*), while unfolding monitored by far-UV CD spectroscopy clearly reveals three state unfolding. In the case of G117F, both CD spectroscopy and fluorescence provide no evidence for an intermediate in the unfolding pathway.

To study site specific equilibrium unfolding, G117F was incubated in various concentrations of GdnHCl at pH 7.8 for 1 h to attain equilibrium. After that, the protein was pulsed for 10 s with D_2O buffer (25 °C, pD 7.8) containing the same concentration of GdnCl as that of the preincubated samples. Under these conditions, amide hydrogens in unfolded regions of the molecule will undergo nearly complete exchange, while hydrogens in folded regions will remain largely protected. This type of pulse labeling experiment has been shown to be an effective method for monitoring site specific folding and unfolding in proteins.

Figure 3 shows the MS spectra of peptide 38−60 in the presence of 0.5, 1.4, and 3.4 M guanidine. At 0 M GdnCl, only one mass envelope was noted. At 1.4 M GdnCl, two peaks of equal intensity were observed, one at a lower and the other at a higher m/z value. The appearance of such bimodal peaks indicates that both folded and unfolded states are populated. As the concentration of the denaturant was increased, intensity of the peak at lower m/z started to decrease and disappeared above 3 M. Therefore, G117F was completely unfolded above 3 M guanidine. The unfolded population at each denaturant concentration was calculated as described in Materials and Methods and plotted against denaturant concentration. The transition midpoint obtained from the unfolding curve, fitted to a two state transition model (Figure 4), matched well with that obtained from CD spectroscopic measurements. We performed similar analysis on all peptides obtained from peptic digests of G117F (Table 1). Because of noise caused by the presence of denaturant, some peptide signals were suppressed, and we present results for 13 peptides covering 42% of G117F. These peptides are, however, well distributed throughout the structure. The unfolding curves for all peptides followed a two state transition with

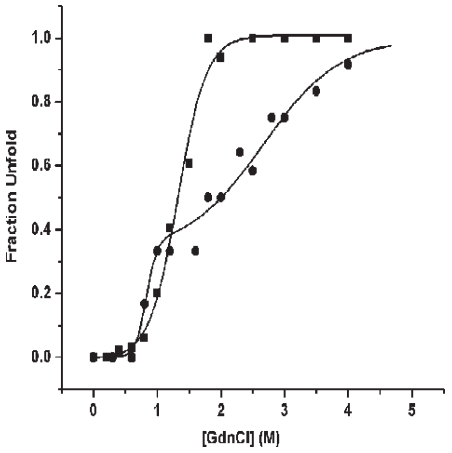

FIGURE 2: GdnHCl induced equilibrium unfolding curves of wild type (●) and G117F (■) α_1AT as measured by CD spectroscopy. The far-UV CD signals were measured for samples equilibrated in varying concentrations of GdnHCl. Data for wild type are reproduced from ref *16*.

midpoints clustered very tightly around 1.4 M GdnCl, in good agreement with the midpoint of 1.4 M obtained from fitting the CD unfolding curve of G117F, but significantly higher than the midpoint of 0.8 M for the native → molten globule transition in wild type. The coincidence of the unfolding curves determined from HXMS and CD indicates that, unlike wild type, G117F unfolds via a single cooperative transition in which both stable hydrogen bonding and secondary structure are lost simultaneously. Stabilization against chemical denaturation is increased quite uniformly throughout the structure. Denaturation midpoints are clustered around a median GdnHCl concentration of 1.4 M with a standard deviation of 0.3 M. This is 0.55 M higher than the average transition midpoint of 0.85 M observed for wild type (*16*). A note about these transition midpoints is in order. We are comparing denaturation midpoints determined by HXMS. However, it was shown previously (*16*) that, for wild type α_1AT, HXMS detects only the first of the two transitions seen by CD. Thus, we are here comparing the wild type native → molten globule transition with the G117F native → fully unfolded transition. Despite this complication, the fact that all peptides studied show a remarkably similar increase in their denaturation midpoints indicates that the effects of the G117F substitution are distributed fairly uniformly throughout the structure. Using the denaturation m-value of 7.9 kcal/mol·M from ref *12*, we can calculate $\Delta\Delta G$ values for all peptides: these cluster around a median value of 4.2 kcal/mol. As with the shifts in transition midpoints, these $\Delta\Delta G$ values should be interpreted with caution, as they represent differences in ΔG between two qualitatively different transitions (native → molten globule and native → fully unfolded).

In addition to examining the effects of the G117F substitution on the unfolding mechanism, we also probed the effects of the Gly → Phe substitution on the conformational dynamics of the native state. We investigated the distribution of flexibility and rigidity in the mutant by H/D exchange mass spectrometry in order to assess the structural differences from the wild type. H/D exchange was performed over a period of 3000 s at pD 7.8 at 25 °C followed by HPLC-MS to quantify the mass of peptic fragments. Clear differences in rates of deuterium uptake are evident in several regions of α_1AT. Figure 5 shows normalized deuterium uptake in the peptic fragment consisting of residues

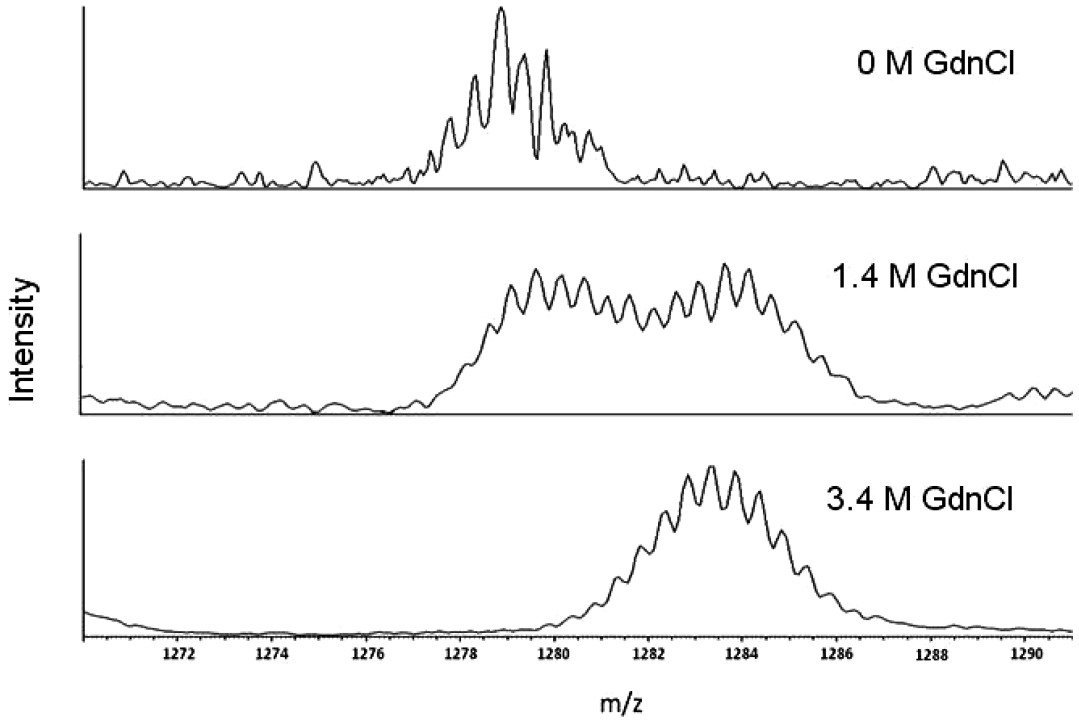

FIGURE 3: MS spectra of a representative peptic fragment 38−60 deuterated in 0 M (top), 1.4 M (middle), and 3.4 M GdnCl.

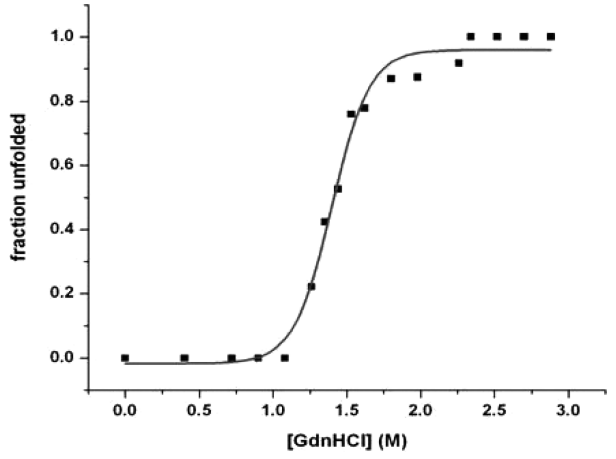

FIGURE 4: Equilibrium unfolding curve for peptic fragment 38−60 determined by H/D exchange mass spectrometry. The curve was fit to a two-state transition model.

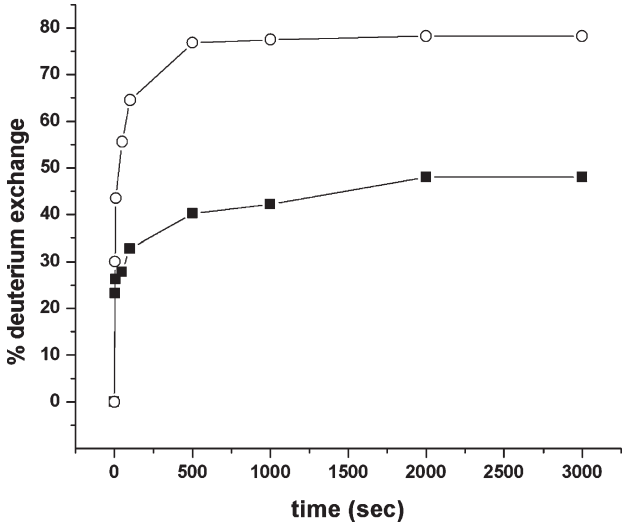

FIGURE 5: Raw data showing the percent deuterium exchange at different time points for the peptide fragment 190−208 derived from the wild type (○) and G117F (■) α_1-AT.

Table 1: Denaturation Midpoint of Each Peptic Fragment Determined by Hydrogen−Deuterium Exchange Mass Spectrometry

residues	[GdnCl]1/2 (M)
38−60	1.41
64−77	1.41
64−84	1.37
85−99	1.40
127−142	1.40
131−142	1.42
143−159	1.33
160−171	1.34
160−172	1.34
209−227	1.33
318−338	1.36
325−338	1.40
352−372	1.40

190−208 for both wild type (open circles) and G117F (filled squares). By 500 s of incubation, the extent of deuterium uptake in wild type is ~35% greater than that in G117F.

Differences in normalized deuterium uptake between G117F and wild type at 10, 100, and 1000 s are shown for all peptides in Figure 6. Noticeable differences in flexibility were observed in peptides 160−171 and 160−172 containing six and seven residues in the C-terminal region of the F helix. In the wild type, this region showed exchange behavior comparable to that observed for unstructured surface loops such as the RCL. Exchange reached more than 80% in 100s time for the wild type, whereas it took 1000 s to show 85% deuterium exchange in G117F. Changes in the flexibility of the F helix were anticipated as the mutation fills a cavity between the F helix and β strand A. Significant changes were also seen in other regions of the

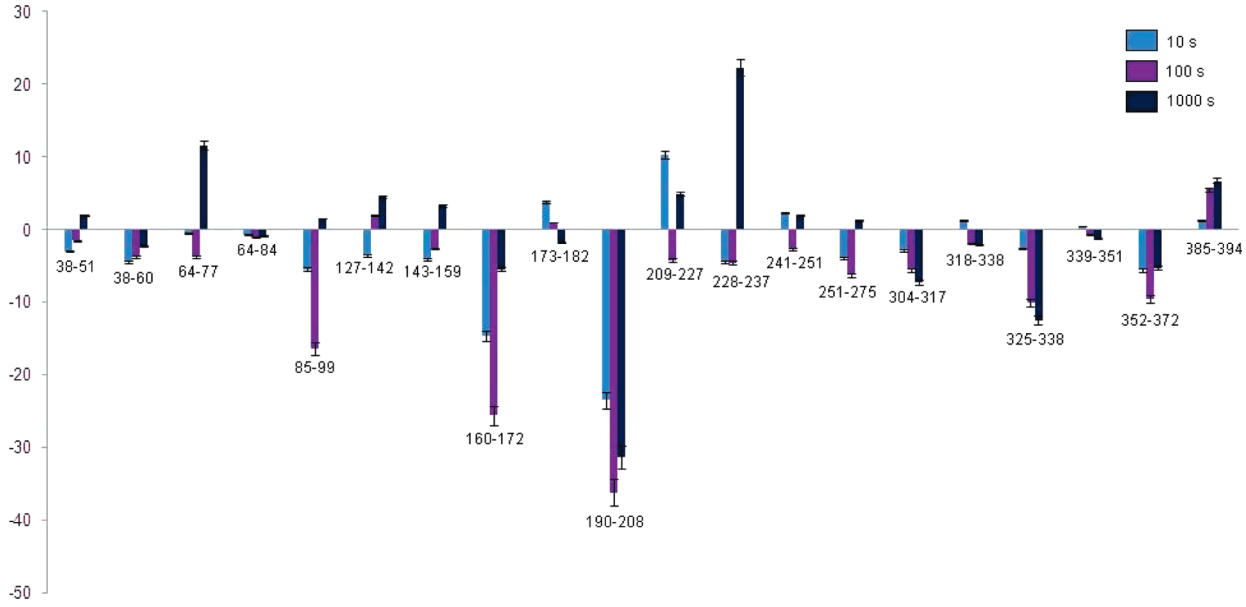

FIGURE 6: Difference in normalized deuterium exchange in G117F relative to wild type. For each peptic fragment, differences are shown for 10 s (light blue bars), 100 s (purple bars), and 1000 s (dark blue bars) incubation in D_2O.

molecule. β-strands 5A (325−338), 1C (352−372), and 4C (190−208) all showed reduced exchange compared to that of the wild type. The top of strand 5A, together with the top of strand 3A, comprises the breach region, which serves as the initial site of RCL insertion. Unfortunately, we lacked coverage in strand 3A and therefore were unable to determine whether the entire breach region is stabilized in G117F.

In addition to helix F, parts of helix I (304−317) and helix D (85−99) also exhibited lower deuterium uptake than wild type. There are also some secondary structures in the mutant showing greater exchange behavior compared to that of the wild type. Residues 228−237 (comprising β1B and some unstructured surface loops) and 64−77 (comprising a loop and a portion of helix C) showed higher exchange behavior compared to that of the wild type at longer time points, although this showed less exchange at shorter time points. A plausible explanation for this behavior is that the least protected amide hydrogens in these regions (those that chiefly contribute to exchange at short labeling times) have been stabilized by the G117F substitution, while those amide hydrogens that are the most strongly protected against exchange are somewhat destabilized. Residues 385−395 also show slightly increased exchange at both short and long labeling times. Figure 7 represents the different structural regions of α_1AT which show significant changes in native state dynamics due to mutation. Conformational dynamics in other parts of the molecule remained more or less similar to that of the wild type.

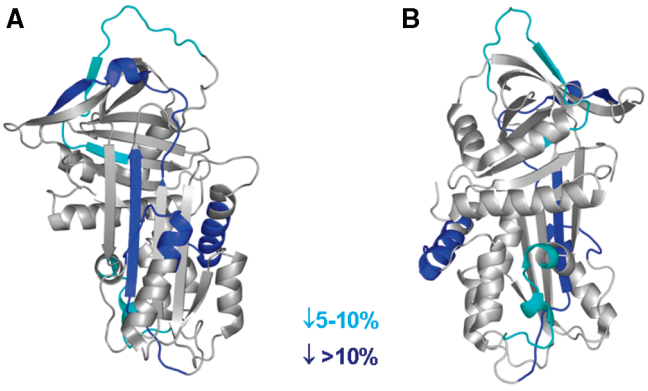

FIGURE 7: Relative deuterium levels at 100 s in G117F compared to that of wild type mapped onto the three-dimensional structure of α_1AT. Both front (A) and back (B) views of the structure are shown. The figures were prepared using PyMol (*38*).

DISCUSSION

It was previously demonstrated that the G117F substitution increases the stability of the metastable form of α_1AT. Employing HXMS, we have found that this substitution also completely alters the unfolding mechanism. It is remarkable that a single amino acid substitution is sufficient to abolish the molten globule intermediate during equilibrium unfolding from the metastable state to the unfolded state. While position 117 has relatively low solvent accessibility, it cannot be considered as occupying the core of α_1AT. Position 117 lies on the outside of β-sheet A, and the phenylalanine side chain will face outward, interacting primarily with the F-helix as revealed by the crystal structure (*21*).

Furthermore, the G117F substitution alters the unfolding mechanism not primarily by stabilizing the native state (although there is some stabilization relative to the native → molten globule transition of the wild type) but by destabilizing the unfolding intermediate (Figure 2). At 2.5 M GdnHCl, for example, G117F is already fully unfolded as judged by CD, but the wild type still retains considerable secondary structure. This is especially surprising since the introduction of a large nonpolar Phe side chain would, if anything, be expected to stabilize a compact denatured state. How this destabilization of the molten globule is achieved is unclear. Presumably, the Phe side chain must disrupt stabilizing interactions in the intermediate state ensemble. From H/D exchange, we know that the intermediate lacks both stable secondary structure and a well packed hydrophobic core, but this does not rule out local or even long ranged side chain interactions. Lacking detailed information on the structure of the intermediate, we cannot say which specific interactions are disrupted by the G117F substitution. We are aware of one other instance in which 3 state unfolding is eliminated through destabilization of the intermediate rather than stabilization of the native state, and it is notable that this instance involves

another member of the serpin family. The thermophilic serpin thermopin contains a C-terminal extension not found in eukaryotic serpins. Chemical denaturation of thermopin shows 3 state unfolding. Deletion of the 5 C-terminal residues eliminates the unfolding intermediate without substantial stabilization of the native state (*22*).

Seo et al. showed that the accumulation of multiple stabilizing mutations in α_1AT results in activity deficient variants (*14*). They further found that substantial activity loss is accompanied by the disappearance of the unfolding intermediate (seen in the wild type and modestly stabilized mutants) and the onset of two-state rather than three state unfolding. Having demonstrated using H/D exchange and other techniques that the intermediate seen in the three state unfolding of wild type α_1AT is a molten globule, we proposed that the ability to populate a molten globule is correlated with, and perhaps necessary for, efficient protease inhibition by serpins (*16*). We suggested that the reason for this correlation is that α_1AT must undergo transient disruptions throughout the structure, and not just at the loop insertion site, during inhibition. This is also supported by the work of Baek et al. where they used H/D exchange mass spectrometry to show that α_1AT undergoes transient unfolding in several structural regions, including regions distant from the loop insertion site, during protease inhibition (*23*). Now with G117F, we have also demonstrated that decreased activity due to a stabilizing mutation is accompanied by loss of the ability to populate the molten globule state at low concentrations of denaturant. If large scale transient disruption of the folded structure is indeed required for RCL insertion during inhibition, then the altered unfolding observed here could influence activity through two mechanisms. On the one hand, the G117F mutation introduces favorable interactions that stabilize the folded structure. On the other hand, this mutation appears to destabilize the molten globule by an unknown mechanism. Both effects will increase the energetic distance between the folded state and the compact denatured state, thus increasing the energy barrier to be surmounted during the inhibitory conformational change (if in fact α_1AT must pass through a compact denatured state during inhibition).

We note that the effects of the G117F mutation are not identical for all denaturants. Gooptu et al. found that primary effects of G117F on urea denaturation were to shift the onset of unfolding to higher concentrations (from 0.7 M for the wild type to 2.0 M for G117F) and to shift the midpoint of transition (from 3.4 to 4.3 M) (*21*). There was no clear indication that an unfolding intermediate had been eliminated. This is not surprising given that the unfolding behavior of wild type α_1AT is quite different in urea and GuHCl. When it was monitored by CD spectroscopy, GuHCl denaturation of α_1AT shows a very clear unfolding intermediate in which nearly 70% of the native ellipticity at 222 nm is retained (*19*). In contrast, the unfolding intermediate in urea is much less distinctly resolved by CD (it is more apparent to tryptophan fluorescence) and retains at most ~25% of its native ellipticity at 222 nm (*24*). The unfolding mechanism of α_1AT (and perhaps other serpins) thus shows unusual plasticity: the intermediates populated (or not) and the degree of structure they retain can be significantly altered either by changing the denaturant employed or by amino acid substitutions.

In addition to its effects on the unfolding mechanism, the G117F substitution also affects local conformational dynamics. On the basis of the location of position 117 and the expected contacts between the F helix and the Phe side chain, the significant reduction in flexibility seen in the C-terminal half of the F helix is not surprising. On the basis of crystal structures, the F helix blocks the path traversed by the RCL during translocation and must be physically displaced in order for complete loop insertion to occur. Therefore, it has an important role in serpin function (*25*−*31*). Previous H/D exchange data on wild type α_1AT showed that the top of the F helix is highly dynamic in solution, indicating weak interactions with β sheet A (*15*). It was suggested that these weak interactions would facilitate easy displacement of the F helix and thus allow efficient loop translocation. The recently published 3.2 Å crystal structure of G117F showed that the F helix is shifted toward the bottom of the β sheet 3A by half a turn. Also, introduction of the extra aromatic ring (Phe 117) into the helix F−β sheet A interface increases favorable packing interactions ultimately leading to the stabilization of helix F (*21*). This might also retard loop translocation (as the F helix is more difficult to move aside) in G117F, thus leading to decreased activity.

Despite the fact that the crystal structure of G117F indicates no significant conformational changes other than those in and around the F helix, we find that distant regions show altered dynamics in G117F. This is consistent with the proposition that allosteric communication between distant protein regions can occur without a discrete conformational change (*32*). Interestingly, the effects of the substitution are not uniformly distributed in the structure, despite the global effect on the unfolding mechanism, and in much of the structure, native state dynamics are not significantly altered by the mutation. Although in the crystal structure no significant changes were seen in β sheet A or β sheet C (*21*), regions showing significant changes in H/D exchange behavior include strand 5A, strands 1 and 4C, and helix D. They all show reduced flexibility/increased stability in G117F. Strand 5A makes contacts with residues on the loop C terminal to the F helix, which, in turn, makes contacts with the F helix itself. Stabilization could propagate through these interactions. More surprising is the significant stabilization of β strands 1C and 4C. These are ≥40 Å from position 117 and make no contacts with helix F or strand 5A.

Except for strand 4C, all of the significantly affected regions are involved in regulating or propagating conformational changes, either in α_1AT or in other serpins. Strand 5A is part of the breach region and must separate from strand 3A during RCL insertion. The release of strand 1C from the rest of sheet C is critical for both the native → latent transition and for polymerization (*33*). G117F shows retarded polymerization in addition to decreased activity against some proteases (*21*). The most obvious explanation for this is strengthened interaction between the F helix and the face of β sheet A, as seen in the crystal structure. Our results suggest that stabilization of strand 1C may also contribute to retarded polymerization. Additionally, the observed stabilization of strand 5A is also consistent with retarded polymerization. Increased stability in strand 5A might discourage polymerization by making it more difficult to separate from strand 3A (in the loop sheet model of polymerization) or by making it more difficult to entirely expel strand 5 from sheet A (in the recently proposed domain swap model of polymerization (*34*)). In serpins such as antithrombin, helix D plays a key role in allosteric activation; the effects of heparin binding to helix D are transmitted to the breach region and result in expulsion of the partially inserted RCL (*4*). Finally, large displacements are required of helix F during RCL insertion (*30*). The fact that the dynamic effects of the G117F substitution are concentrated in these functionally important regions suggests that they may

form a network of dynamically and energetically coupled residues. Such coupling would facilitate the propagation of conformational changes between different regions of the molecule.

Proteins in solution exist as statistical ensembles, sampling many different conformations more or less frequently based on their relative energies. Hilser et al. have proposed that both local stability/flexibility and long-range cooperative interactions in proteins are mediated by the global protein ensemble (*35*). In the context of ligand binding and allostery, this approach suggests that instability is critically important for the propagation of binding induced structural changes to distant regions in a protein's structure. Ensemble based models indicate that binding effects are propagated to distant regions most efficiently if a portion of the binding site is highly unstable in the absence of ligand and is stabilized upon ligand binding (*36*). This ensemble based view may aid in understanding the dramatic global effects of the G117F substitution in α_1AT. Previous H/D exchange studies of wild type α_1AT found that the top of the F helix is one of the most unstable regions of the molecule, exchanging at rates comparable to that of an unstructured loop. The effect of introducing a Phe side chain at position 117 can be thought of as analogous to ligand binding to an unstable binding site in that it forms contacts with the F helix and dramatically stabilizes it. Such stabilization would lead to a redistribution of the native state ensemble in a manner similar to that proposed for allosteric ligand binding. Applying an ensemble based computational algorithm to a large set of enzymes, Lui et al. also found that functional residues showed stronger energetic coupling to the rest of the molecule than nonfunctional residues (*37*). α_1AT is not an enzyme, and therefore, the functional residues are not easily defined. α_1AT's function requires a massive conformational change involving much of the molecule, and the intensive mutagenesis efforts of Yu et al. have established that functional residues are in fact distributed throughout the structure (*10*). This unusual property of α_1AT (and perhaps of inhibitory serpins in general) may explain the unusually strong energetic coupling whereby local stabilizing interactions between sheet A and the F helix propagate to distant regions and eliminate cooperative unfolding to the molten globule intermediate at low concentrations of denaturant.

This perspective in which energetic coupling between local regions is mediated by the overall protein ensemble suggests that both local and global changes in stability contribute to decreased activity against trypsin and elastase. Locally, strengthened interactions between the F helix and β-sheet A will make displacing the F helix more difficult, thus retarding loop insertion. However, this strengthened F helix−sheet A interaction modulates the entire ensemble of α_1AT, increasing the thermodynamic stability of the active state and apparently decreasing the stability of the compact intermediate. If distributed transient unfolding is required during the inhibitory transition, as the work of Baek et al. suggests (*23*), then this reordering of the relative stability of states will also retard loop insertion by increasing the energy barrier that must be overcome.

ACKNOWLEDGMENT

We thank Dr. Anne Gershenson (Brandeis University) for providing the plasmid encoding the G117F mutant of α_1AT.

REFERENCES

1. Potempa, J., Korzus, E., and Travis, J. (1994) The serpin superfamily of proteinase inhibitors: structure, function, and regulation. *J. Biol. Chem. 269*, 15957–15960.
2. Huber, R., and Carrell, R. W. (1989) Implications of the three-dimensional structure of alpha 1-antitrypsin for structure and function of serpins. *Biochemistry 28*, 8951–8966.
3. Stratikos, E., and Gettins, P. G. (1999) Formation of the covalent serpin-proteinase complex involves translocation of the proteinase by more than 70 Å and full insertion of the reactive center loop into β-sheet A. *Proc. Natl. Acad. Sci. U.S.A. 96*, 4808–4813.
4. Gettins, P. G. (2002) Serpin structure, mechanism, and function. *Chem. Rev. 102*, 4751–4804.
5. Lee, K. N., Park, S. D., and Yu, M. H. (1996) Probing the native strain in alpha 1-antitrypsin. *Nat. Struct. Biol. 3*, 497–500.
6. Lee, K. N., Im, H., Kang, S. W., and Yu, M. H. (1998) Characterization of a human alpha 1-antitrypsin variant that is as stable as ovalbumin. *J. Biol. Chem. 273*, 2509–2516.
7. Im, H., Seo, E. J., and Yu, M. H. (1999) Metastability in the inhibitory mechanism of human alpha 1-antitrypsin. *J. Biol. Chem. 274*, 11072–11077.
8. Ryu, S. E., Choi, H. J., Kwon, K. S., Lee, K. N., and Yu, M. H. (1996) The native strain in the hydrophobic core and flexible reactive loop of a serine protease inhibitor: crystal structure of a uncleaved alpha 1-antitrypsin at 2.7 Å. *Structure 4*, 1181–1192.
9. Lomas, D. A., Evans, D. L., Finch, J. T., and Carrell, R. W. (1992) The accumulation of Z alpha 1-antitrypsin in liver. *Nature 357*, 605–607.
10. Seo, E. J., Im, H., Maeng, J. S., Kim, K. E., and Yu, M. H. (2000) Distribution of the native strain in human alpha 1-antitrypsin and its association with protease inhibitor function. *J. Biol. Chem. 275*, 16904–16909.
11. Im, H., and Yu, M. H. (2000) Role of Lys 335 in the metastability and function of inhibitory serpins. *Protein Sci. 9*, 934–941.
12. Lee, C., Park, S. H., Lee, M. Y., and Yu, M. H. (2000) Regulation of protein function by native metastability. *Proc. Natl. Acad. Sci. U.S.A. 97*, 7727–7731.
13. Lee, C., Maeng, J. S., Kocher, J. P., Lee, B., and Yu, M. H. (2001) Cavities of alpha (1)-antitrypsin that play structural and functional roles. *Protein Sci. 10*, 1446–1453.
14. Seo, E. J., Lee, C., and Yu, M. H. (2002) Concerted regulation of inhibitory activity of alpha 1-antitrypsin by the native strain distributed throughout the molecule. *J. Biol. Chem. 277*, 14216–14220.
15. Tsutsui, Y., Liu, L., Gershenson, A., and Wintrode, P. L. (2006) The conformational dynamics of a metastable serpin studied by hydrogen exchange and mass spectrometry. *Biochemistry 45*, 6561–6569.
16. Tsutsui, Y., and Wintrode, P. L. (2007) Cooperative unfolding of a metastable serpin to a molten globule suggests a link between functional and folding energy landscapes. *J. Mol. Biol. 371*, 245–255.
17. Parfrey, H., Mahadeva, R., Ravenhill, N. A., Zhou, A., Dafforn, T. R., Foreman, R. C., and Lomas, D. A. (2003) Targeting a surface cavity of α_1-antitrypsin to prevent conformational disease. *J. Biol. Chem. 278*, 33060–33066.
18. Devlin, G. L., Chow, M. K., Howlett, G. J., and Bottomley, S. P. (2002) Acid denaturation of alpha 1-antitrypsin: characterization of a novel mechanism of serpin polymerization. *J. Mol. Biol. 324*, 859–870.
19. James, E. L., Whisstock, J. C., Gore, M. G., and Bottomley, S. P. (1999) Probing the unfolding pathway of alpha 1-antitrypsin. *J. Biol. Chem. 274*, 9482–9488.
20. Tew, D. J., and Bottomley, S. P. (2001) Probing the equilibrium denaturation of the serpin alpha 1-antitrypsin with single tryptophan mutants; evidence for structure in the urea unfolded state. *J. Mol. Biol. 313*, 1161–1169.
21. Gooptu, B., Miranda, E., Nobeli, I., Mallya, M., Purkiss, A., Leigh Brown, S. C., Summers, C., Phillips, R. L., Lomas, D. A., and Barrett, T. E. (2009) Crystallographic and cellular characterization of two mechanisms stabilizing the native fold of alpha (1)-antitrypsin: implications for disease and drug design. *J. Mol. Biol. 387*, 857–868.
22. Irving, J. A., Cabrita, L. D., Rossjohn, J., Pike, R. N., Bottomley, S. P., and Whisstock, J. C. (2003) The 1.5 Å crystal structure of a prokaryote serpin: controlling conformational change in a heated environment. *Structure 11*, 387–397.
23. Baek, J., Yang, W. S., Lee, C., and Yu, M. H. (2009) Functional unfolding of α_1-antitrypsin probed by hydrogen-deuterium exchange coupled with mass spectrometry. *Mol. Cell. Proteomics 8*, 1072–1081.
24. Tew, D. J., and Bottomley, S. P. (2001) Probing the equilibrium denaturation of the serpin α_1-antitrypsin with single tryptophan mutants: evidence for structure in the urea unfolded state. *J. Mol. Biol. 313*, 1161–1169.

25. Vleugels, N., Gils, A., Bijnens, A. P., Knockaert, I., and Declerck, P. J. (2000) The importance of helix F in plasminogen activator inhibitor-1. *Biochim. Biophys. Acta 1476*, 20–26.
26. Bijnens, A. P., Gils, A., Knockaert, I., Stassen, J. M., and Declerck, P. J. (2000) Importance of the hinge region between alpha-helix F and the main part of serpins, based upon identification of the epitope of plasminogen activator inhibitor type1 neutralizing antibodies. *J. Biol. Chem. 275*, 6375–6380.
27. Cabrita, L. D., Whisstock, J. C., and Bottomley, S. P. (2002) Probing the role of the F-helix in serpin stability through a single tryptophan substitution. *Biochemistry 41*, 4575–4581.
28. Cabrita, L. D., Dai, W., and Bottomley, S. P. (2004) Different conformational changes within the F-helix occur during serpin folding, polymerization, and proteinase inhibition. *Biochemistry 43*, 9834–9839.
29. Baek, J. H., Im, H., Kang, U. B., Seong, K. M., Lee, C., Kim, J., and Yu, M. H. (2007) Probing the local conformational change of α1-antitrypsin. *Protein Sci. 16*, 1842–1850.
30. Gettins, P. G. (2002) The F-helix plays an essential, active role in the proteinase inhibition mechanism. *FEBS Lett. 523*, 2–6.
31. Zheng, X., Wintrode, P. L., and Chance, M. R. (2008) Complementary structural mass spectrometry techniques reveal local dynamics in functionally important regions of a metastable serpin. *Structure 16*, 38–51.
32. Tsai, C. J., Del Sol, A., and Nussinov, R. (2008) Allostery: absence of a change in shape does not imply that allostery is not at play. *J. Mol. Biol. 378*, 1–11.
33. Chang, W. S., Whisstock, J., Hopkins, P. C., Lesk, A. M., Carrell, R. W., and Wardell, M. R. (1997) Importance of the release of strand 1C to the polymerization mechanism of inhibitory serpins. *Protein Sci. 6*, 89–98.
34. Yamasaki, M., Wei, L., Johnson, D., and Huntington, J. A. (2008) Crystal structure of a stable dimer reveals the molecular basis of serpin polymerization. *Nature 455*, 1255–1258.
35. Hilser, V. J., García-Moreno, E., B., Oas, T. G., Kapp, G., and Whitten, S. T. (2006) A statistical thermodynamic model of the protein ensemble. *Chem. Rev. 106*, 1545–1558.
36. Freire, E. (1999) The propagation of binding interactions to remote sites in proteins: analysis of the binding of the monoclonal antibody D1.3 to lysozyme. *Proc. Natl. Acad. Sci. U.S.A. 96*, 10118–10122.
37. Liu, T., Whitten, S. T., and Hilser, V. J. (2007) Functional residues serve a dominant role in mediating the cooperativity of the protein ensemble. *Proc. Natl. Acad. Sci. U.S.A. 104*, 4347–4352.
38. DeLano, W. L. (2002) The PyMOL Molecular Graphics System, DeLano Scientific, San Carlos, CA, http://www.pymol.org.